Uluslararası İleri Doğa Bilimleri ve Mühendislik Araştırmaları Dergisi
Sayı 7, S. 281-289, 7, 2023

Araştırma Makalesi

IJANSER
https://as-proceeding.com/index.php/ijanser
ISSN: 2980-0811

International Journal of Advanced Natural Sciences and Engineering Researches
Volume 7, pp. 281-289, 7, 2023

Research Article

Improved reliability of Electric Vehicle (EV) charging by using multiport triple active bridge (TAB) converter

Asfer Rasool[*], Engr. Muhammad Ahmad Khurshid [1], Tahir Mehmood [2]

[*]*Electrical Engineering department, UET Taxila , Pakistan*
[1] *Electrical Engineering department, UET Taxila , Pakistan*

[*]*Asfer.rasool@students.uettaxila.edu.pk*

(Received: 25 August 2023, Accepted: 29 August 2023)

(1st International Conference on Recent and Innovative Results in Engineering and Technology ICRIRET 2023, August 16-18, 2023)

ATIF/REFERENCE: Rasool, A., Khurshid, M. A., Ahmad, I. & Mehmood, T. (2023). Improved reliability of Electric Vehicle (EV) charging by using multiport triple active bridge (TAB) converter, *International Journal of Advanced Natural Sciences and Engineering Researches*, 7(7), 281-289.

Abstract **–** The integration of battery energy storage systems (BESS) in EV charging stations (ECS) is gaining popularity as a means to achieve better charging rates while also providing the potential for peak-demand shaping. However, the introduction of an extra conversion stage like in dual active bridge (DAB) converter to facilitate the integration of the BESS results in an increase in system losses, size, and cost . The Triple Active Bridge (TAB) converter shows superior performance compared to the Dual Active Bridge (DAB) converter due to its flexible multiport configuration, which facilitates bidirectional power transfer between different sources and loads, hence boosting the flexibility of the system. The architectural design employed in this context aims to minimise the number of conversion stages, hence mitigating losses and optimising the paths for energy transmission. Consequently, the TAB converter emerges as a superior and versatile solution for integrated energy systems (IES). By directly connecting the BESS to one of these ports, a separate DC-DC converter is no longer required to convert energy between the BESS and the main DC bus. Consequently, the power losses incurred by the converter are diminished, resulting in smaller-sized converters and increased system efficiency. This study presents a proposal for a DC/DC multiport converter that enables the integration of battery storage in ECS using a TAB converter, while still meeting the necessary isolation requirements for ECS.

Keywords – Triple Active Bridge Converter, Multiwinding Transformer, Battery Storage System, EV Charging Stations, MATLAB

I. INTRODUCTION

Efforts have been undertaken in recent years to shift energy production away from fossil fuels and towards renewable energy sources, as well as to incentivise the use of low-emission automobiles. Battery electric vehicles (BEVs) and hybrid electric vehicles (HEVs) are among the most promising types of low-emission vehicles, with significant increase projected over the next several years. It is critical to provide consumers with dependable and widely available charging infrastructure in order to raise their adoption rates. Furthermore, it is critical to build EV charging stations (ECS) to reduce the charging time of BEVs and also to reduce range

anxiety so that they can compete with internal combustion engines (ICE) [1].

The massive power consumption of a widespread ECS network, on the other hand, poses a danger to grid stability due to its unpredictable nature [2]. Battery electric vehicles (BEVs) rely exclusively on a high-capacity traction battery pack for their power, which is recharged through the use of an electrical supply. Plug-in hybrid electric vehicles (PHEVs) are equipped with a battery pack that is comparatively smaller in size, in addition to an internal combustion engine (ICE) [9,10]. The batteries of both hybrid electric vehicles (HEVs) and fuel cell electric vehicles (FCEVs) are not charged directly from the utility grid [3]. Hence, the establishment of a robust charging infrastructure assumes paramount importance for Battery Electric Vehicles (BEVs) as opposed to Plug-in Hybrid Electric Vehicles (PHEVs) owing to the larger battery capacity and absence of alternate power sources. These four types make most of the market of electric vehicles (EV's) shown in Figure 1. Hence, the utilization of batteries or supercapacitors to accommodate the need for rapid responsiveness in EVs and various other applications [4]. EVs have the option to utilize several energy storage technologies, such as lithium-ion batteries, supercapacitors, fuel cells, or a combination of these, in order to enhance power density. The integration of various forms of energy and storage enables the transformation of electrical systems into integrated energy systems (IES) [5].

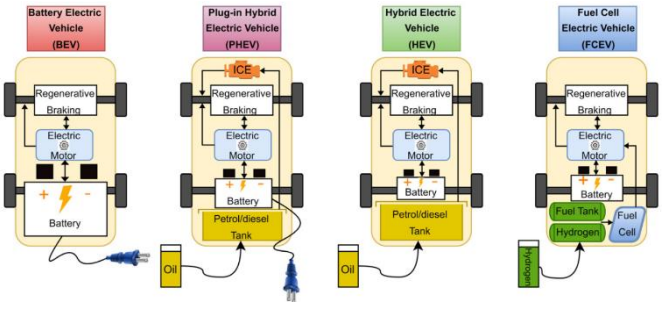

Figure 1: Four basic types of EV's

The integration of BESS in EV charging stations (ECS) has garnered significant attention due to its ability to reduce peak power during the charging process [6]. In addition, the use of BESS results in a decrease in the necessary grid connection capacity. This holds particular significance in areas where the existing local electricity infrastructure may not possess the capacity to support the attainment of high powers at the ECS. The absence of a BESS in the ECS necessitates a costly update of the current power grid infrastructure [7], which may not yield a favourable cost-benefit.

There are two primary variables that contribute significantly to the economic viability of integrating BESS into ECS. Firstly, there has been a consistent decrease in the prices associated with battery storage. Secondly, there are large number of second life batteries, these batteries have been removed from EVs once their capacity falls below 80% of their initial value [8], [9].

The literature discusses many ways for integrating BESS in FCS. One often employed strategy is incorporating the Battery Storage System (BESS) into the Direct Current (DC) Link by means of an extra DC/DC converter, as depicted in Figure 1 (a).

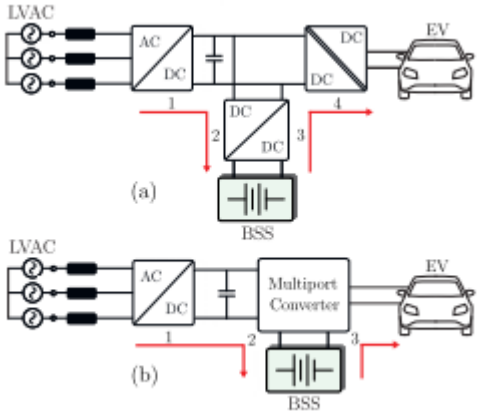

Figure 2:Two architectures are proposed for combining the Battery Energy Storage System (BESS) with the necessary converters to charge the EV from the BESS and the grid. (a) Integrates the BESS in the DC link (b) integrates it with a multiport converter.

Because of its exceptional conversion efficiency and excellent power density, the integration of Battery Energy Storage Systems (BESS) employing a multiport converter, as shown in Figure 1 (b), is gaining popularity. As seen in Figure 1, using a multiport converter architecture provides substantial benefits, owing to its ability to improve round-trip efficiency. This benefit stems from the system's reduced number of conversion stages. Dual Active Bridge (DAB) and Triple Active Bridge (TAB) converters are well-known examples of

isolated bidirectional converters. More information about the features of these converters can be found in [10]

The dual active bridge (DAB), which is an isolated bidirectional dc-dc converter, has been suggested for numerous applications [11]. The DAB converter consists of two full-bridge inverters that are interconnected through an isolation transformer during high-frequency operation, as depicted in Figure 2 [12]. One of the advantages of this system is its ability to facilitate bidirectional power transfer while maintaining a high level of efficiency. However, the limitation is in its ability to link just two ports. Consequently, multiple DAB converters are required to establish connections between various components and the DC-bus in the IES. Additionally, it may be necessary to implement a communication bus in order to regulate the flow of electricity.

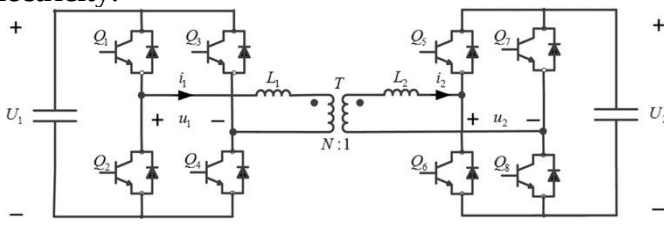

Figure 3: Dual active bridge (DAB) converter

The Triple Active Bridge (TAB) converter is a multiport version of the Dual Active Bridge (DAB) converter. The TAB converter concept is to extend the capabilities of the DAB converter by incorporating an additional port, as shown in Figure 3.

This enhancement allows the TAB converter to inherit the benefits of the DAB converter. The breadth of this technology, however, extends beyond simply one more port, as it provides adaptable power transfer over three unique ports, as seen in Figure 3. This advancement demonstrates the possibility for improved power management and efficient energy transfer among these numerous ports, supporting a more complex approach to power electronics. The diagram in Figure 3 demonstrates the necessity of deploying three DAB converters in order to facilitate adaptable power transmission across three components.

In contrast, Figure 3b achieves the same objective with only a single TAB converter. Furthermore, the need for communication among the three elements is not essential while utilizing the TAB converter. Hence, the management of the entire system is more direct.

Furthermore, as compared to conventional multiport converters, the TAB converter offers a distinct benefit through the utilization of a transformer. This transformer not only facilitates the conversion of voltage ratios but also enhances the overall safety of the system. Hence, the TAB converter is being suggested for numerous applications in the fields of integrated energy systems (IES) and direct current (DC) grids[13].

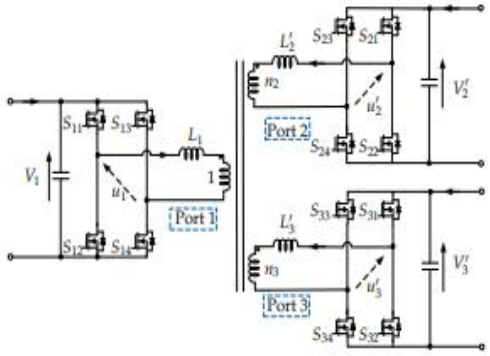

Figure 4: Triple active bridge (TAB) converter

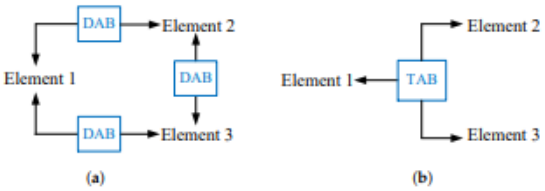

Figure 5:System comparison of TAB and DAB (a) DAB conveter as a system (b) TAB converter as a system

II. Proposed Topology

There are three main sections in the circuit: the DC/AC segment, the high-frequency isolation module, and the AC/DC component. The elements of the DC/AC section include a dc-link capacitor and a complete bridge. The high-frequency isolation section revolves around the high-frequency transformer, whereas the AC/DC module includes a full bridge and dc-link capacitor. Here, N represents the transformer ratio, and L1 and L2 represent the leakage inductance of transformer T.

In a ideal case, the dc-link capacitor and complete bridge combine to form a three-level voltage source. Simultaneously, the high-frequency transformer (without the excitation inductance) can be seen as a leakage inductance. As a result of this reduction, we may create the Dual Active Bridge

(DAB) equivalent circuit on the primary side, as shown in Figure 6. where $i_2' = (i_{2/N}) = i_1$, $u_2' = Nu_2$ and the inductor $L = (L_1 + N^2 L_2)$ acts as a power transfer component, and power flows from the voltage's leading to lagging side respectively[15].

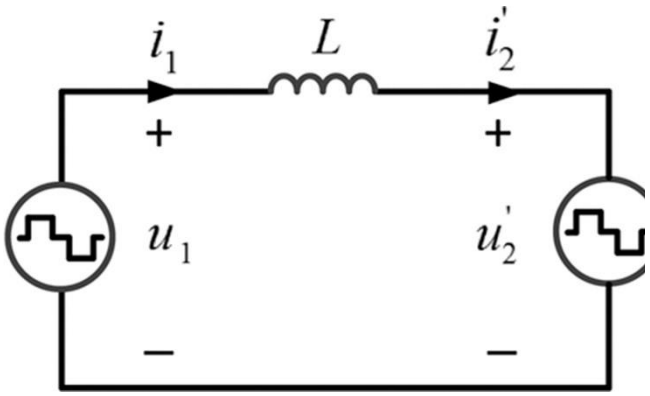

Figure 6:DAB converter Equivalent circuit

The Single Phase Shift (SPS) control method for the Dual Active Bridge (DAB) converter is a well-known and widely used conventional modulation strategy. Both u_1 and u_2 are simplified into two-level square waveforms that consistently show a duty cycle of 50% in this manner. Figure 7 is a visual representation of this concept. Given that u_1 is at an angular location that surpasses u_2 by an angle, where is within the range [0,1], the following approach can be used to calculate the resultant steady-state current i_1 within a single switching cycle Ts[15].

$$i_1(t) = \begin{cases} \frac{(1-2\varphi)U_2' - U_1}{4L} T_s + \frac{U_1 + U_2'}{L} t, & t \in \left[0, \frac{\varphi T_s}{2}\right) \\ \frac{U_2' - (1-2\varphi)U_1}{4L} T_s + \frac{U_1 + U_2'}{L}\left(t - \frac{\varphi T_s}{2}\right), & t \in \left[\frac{\varphi T_s}{2}, \frac{T_s}{2}\right) \\ -i_1\left(t - \frac{T_s}{2}\right), & t \in \left[\frac{T_s}{2}, T_s\right) \end{cases} \quad (1)$$

The application of this SPS control technique not only provides significant insights into the DAB converter's working characteristics, but also aids in the development of a fundamental understanding of the relationship between u1, u2, and the ensuing current dynamics. Based on the information provided in equation (1), it is possible to deduce transmision power characteristics of the DAB converter when operating in the SPS control mode[15]:

$$P = \frac{1}{T_s}\int_0^{T_s} u_1 i_1 \, dt = \frac{U_1 U_2' T_s}{2L}\varphi\,(1-\varphi) \quad (2)$$

The relationship between the transmitted power (P) and the external phase shift angle (φ) is of particular interest due to its quadratic characteristic [16]:

$$\varphi_{1,2} = \frac{1 \pm \sqrt{1-(8LP/U_1 U_2' T_s)}}{2} \quad (3)$$

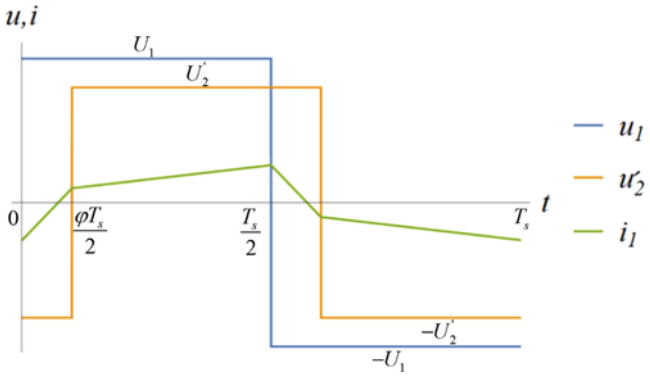

Figure 7:The voltage and current waveforms of the DAB converter in SPS control can be seen.

In accordance with the SPS methodology, the characteristic of the DAB converter exhibiting the highest current stress is as follows[16]:

$$i_{1\max} = \max\left\{|i_1(0)|, \left|i_1\left(\frac{\varphi T_s}{2}\right)\right|\right\} = \begin{cases} \frac{U_2' - (1-2\varphi)U_1}{4L} T_s, U_1 \le U_2' \\ \frac{U_1 - (1-2\varphi)U_2'}{4L} T_s, U_1 > U_2' \end{cases} \quad (4)$$

The rms current stress characteristic of the DAB converter is determined using the SPS methodology and is as follows[16]:

$$i_{1\text{rms}} = \sqrt{\frac{1}{T_s}\int_0^{T_s} i_1^2 \, dt} = \frac{\sqrt{3}T_s}{12L}\sqrt{U_1^2 - 2(1-6\varphi^2+4\varphi^3)U_1 U_2' + U_2'^2} \quad (5)$$

The expression (4) demonstrates that there is a correlation between a decrease in the shift angle and a reduction in the current stress for a given power P. In most cases, we focus on the scenario in which smaller are involved[17]:

$$\varphi = \frac{1 - \sqrt{1-(8LP/U_1 U_2' T_s)}}{2} \in \left[0, \frac{1}{2}\right] \quad (6)$$

When switch Q is in the deactivated condition and current flows in the forward direction, a subsequent

channel becomes accessible. The present electrical flow is directed through the anti-parallel diode D' located within the same branch as switch Q, specifically in conjunction with switch Q'. This phenomena occurs prominently when switch Q' is activated, resulting in a significant decrease in voltage across it to reach zero. Consequently, an interesting phenomenon emerges - the achievement of a state characterised by Zero-Voltage Switching (ZVS) in an open configuration for Q'. The single phase shift (SPS) methodology enables the Dual Active Bridge (DAB) converter to achieve the ZVS state, which reveals an important feature of its operational dynamics.[18]

$$\begin{cases} i_1(0) < 0 \\ i_1(\frac{\varphi T_s}{2}) > 0 \end{cases} \Leftrightarrow \begin{cases} |\varphi| > \frac{1}{2} - \frac{U_1}{2U_2'} \\ |\varphi| > \frac{1}{2} - \frac{U_2'}{2U_1} \end{cases} \quad (7)$$

TAB converter is a DAB converter multi-port extender. According to the study of DAB converter, the inductor is clearly responsible for power transfer between two ports. As a result, in the instance of three The TAB converter is a multi-port DAB converter extension. According to the findings of the DAB converter study, the inductor is critical in easing power transfer between two ports. As a result, when working with a system with three ports, connecting one inductor between each pair of ports makes it easier to achieve bidirectional power transfer. Figure 7a depicts the TAB converter's delta equivalent circuit. The star-delta transformation allows the star configuration to be deduced [19].

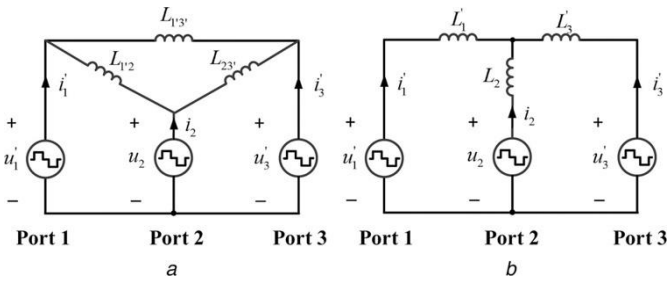

Figure 8: (a) star equivelent TAB converter (b) delta equivlent TAB converter

where

$$\begin{cases} L_{1'2} = L_1' + L_2 + \frac{L_1' L_2}{L_3'} \\ L_{1'3'} = L_1' + L_3' + \frac{L_1' L_3'}{L_2} \\ L_{23'} = L_2 + L_3' + \frac{L_2 L_3'}{L_1'} \end{cases} \quad (8)$$

The TAB converter circuit's configuration, depicted in Figure 8, is derived from the analysis of the star equivalent circuit. It is worth mentioning that the three inductors present in the star equivalent circuit are representative of the intrinsic leakage inductances associated with the three-port transformer [19].

TAB converters utilise the identical Single-Phase Shift (SPS) control mechanism that is comparable to DAB converters. The square wave variables u_1', u_2, and u_3' are characterised by a duty cycle of 50% that is evenly distributed. In the given hypothetical scenario, there is a situation where u_1' is leading u_2 by an angle φ_{12}, as illustrated in Figure 5. Moreover, the vector u_2 is rotated by an angle φ_{23} with respect to the vector u_3', whereas the vector u_1' is ahead of u_3' by an angle φ_{13}. The power transmission features of the TAB converter are elucidated by utilising the triangular equivalent circuit depicted in Figure 6a, in conjunction with the power transmission attributes intrinsic to the DAB converter, as expressed in equation (1):

$$\begin{cases} P_{12} = \frac{U_1' U_2 T_s \varphi_{12}(1-|\varphi_{12}|)}{2L_{1'2}} \\ P_{23} = \frac{U_2 U'_3 T_s \varphi_{23}(1-|\varphi_{23}|)}{2L_{23'}} \\ P_{13} = \frac{U_1' U_3' T_s \varphi_{23}(1-|\varphi_{23}|)}{2L_{1'3'}} \\ P_1 = P_{12} + P_{13} \\ P_2 = -P_{12} + P_{23} \\ P_3 = -P_{13} - P_{23} \\ \\ \\ \varphi_{13} = \varphi_{12} + \varphi_{23} \end{cases} \quad (9)$$

Expression (9) provides an intriguing peek into the complex interplay that governs the gearbox power within the TAB converter. This relationship, in particular, intersects with the phase shift angles φ_{12}, φ_{23}, and φ_{13}, revealing a complex dynamic. The substantial coupling and non-linearity that pervades

the system's behaviour contribute significantly to its complexity.

An fascinating web of relationships arises from this relationship. Linear coupling connects the gearbox power values P_1, P_2, and P_3 to the power values P_{12}, P_{23}, and P_{13}. This dependency emphasises the cooperative character of these variables and their involvement within the operating dynamics of the converter.

A layer of quadratic non-linearity arises as well, enmeshing the powers of P_{12}, P_{23}, and P_{13} with the phase shift angles φ_{12}, φ_{23}, and φ_{13}. This quadratic relationship highlights the subtle interaction between power levels and phase shift modifications, revealing a complex web of relationships.A linear link forms between phase shift angles φ_{12} and $\varphi_{23}$with regard to φ_{13}, in addition to these complexities. This linear relationship represents the smooth evolution of these angles inside the dynamics of the TAB converter, illustrating the comprehensive nature of phase shift adjustments.

Essentially, the multiple relationships represented by expression (9) highlight the complexities of the TAB converter's behaviour. The operational dynamics of the converter are built on these interactions, which are characterised by coupling, non-linearity, and interdependence. This knowledge is a vital resource for engineering endeavours aimed at optimising performance and control tactics in the field of power electronics systems.Given the starting values of φ_{12}, φ_{23} in the interval [0, 1/2], a conclusion can be formed from the insights represented in equation (9). This deduction, in particular, reveals the fundamental link that regulates the shift phase φ_{23}in regard to power dynamics.

Figure 8 is an illuminating visual aid that illustrates this deduction in a real way. This graph vividly depicts the distinct power profiles, P1 and P2, assigned to the converter system's ports 1 and 2. These graphical representations provide a visual picture of the complex interplay between phase changes and power distribution. The complex relationship between the transmission power of the TAB converter ports (P_1, P_2, P_3) and the associated phase shift angles ($\varphi_{12}, \varphi_{23}, \varphi_{13}$) is revealed by expression (9). Because of the system's significant coupling and non-linearity, this connection is quite complex. The interaction consists of a linear coupling interrelationship between the power levels (P_1, P_2, P_3) and (P_{12}, P_{23}, $P1_3$), followed by a quadratic non-linear correlation between (P_{12}, P_{23}, $P1_3$) and $\varphi_{12}, \varphi_{23}, \varphi_{13}$, which is further characterised by a linear correlation between $\varphi_{12}, \varphi_{23}$ and φ_{13}.

In the case where the initial phase shifts φ_{12} & φ_{23} are in the range [0, 1/2], deduction from equation (9) explains the relationship between the phase shiftφ_{23} and power. Figure 8 depicts the respective power profiles (P_1 and P_2) over port 1 and port 2 to illustrate this relationship. This in-depth investigation of the connection between phase shifts and power levels has important implications for comprehending the complex dynamics at work in the setting of the TAB converter [19].

$$
\begin{aligned}
&[(ab+bc+ac)^2-4abc^2]\varphi_{23}^4 \\
&+[2b(ab+bc+ac)(a+c)-4abc^2]\varphi_{23}^3 \\
&+[P_2(4ac^2-2(a-c)(ab+bc+ac))-2aP_1(ab+bc+ac) \\
&+a^2c^2-b^2(a+c)^2]\varphi_{23}^2 \\
&+[P_2(4abc^2+a^2b+bc^2)+P_1(2abc+2a^2b)]\varphi_{23} \\
&-a^2P_1^2-(a^2+2ac)P_1P_2-(a-c)^2P_2^2=0
\end{aligned} \tag{10}
$$

where $a=(U_1'U_2T_s/2L_{1'2}), b=(U_2U_3'T_s/2L_{23'}), c=(U_1'U_3'T_s/2L_{1'3'})$. It can be seen from (10) that the relationship between φ_{23} and P_1, P_2 is quartic. While the quartic equation has a root formula, its solution is quite complicated, making it unsuitable for real-world applications. However, the daunting presence of significant nonlinearity poses its own set of difficulties. This intricacy impedes a thorough examination of current stress and efficiency qualities within the context of the TAB converter, as well as the development of high-performance control techniques. To alleviate these complexities, it is critical to address and mitigate the inherent nonlinearity. The coupling between the various ports can thus be reduced, resulting in a more manageable and cohesive system.

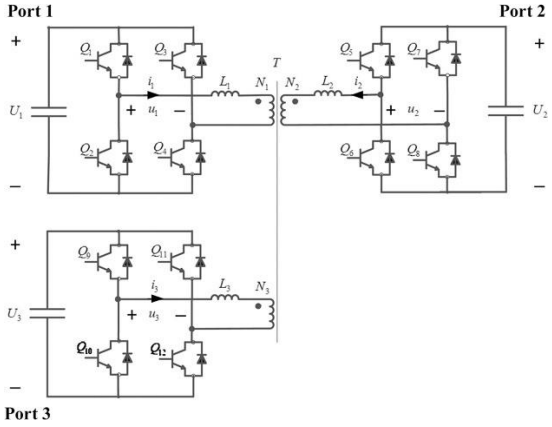

Figure 9: Schematic of TAB converter

A. *TAB Control*

The converters that exhibit the highest level of effectiveness are characterised by meticulously crafted control systems. The control stage assumes responsibility for overseeing and supervising the operation of the system, as well as managing the transfer of energy to and from the surrounding environment. This paper presents an examination of the stability of the system, control parameter determination, and graphical representations. Additionally, frequency-domain simulations are performed. To maintain conciseness, the subsequent illustrations showcase the performance of the single phase shift (SPS) technique for two distinct values of D, namely 0.01 and 0.45 [20].

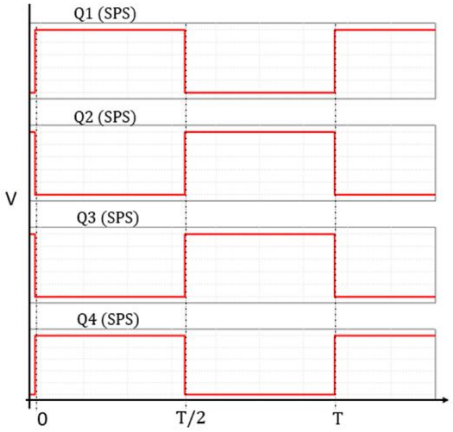

Figure 10: Single phase shift

These techniques offer enhanced system identification and improved comprehension of system activity. Simulating parameters can be seen in table 1.

Specification	Symbol	Value
DC linked voltages (V)	U1, U2, U3	400
Switching frequency (kHz)	f	25-30
Turn ratio	N	1:1:1
Leakage inductance (μH)	L	30
Maximum Power (kW)	P_{max}	14.8
Internal phase shift	φ	30°

Table 1: Simulating parameters

III. RESULTS

MATLAB/Simulink can be seen in figure 11 below. The simulation are the same as discussed in previous section.

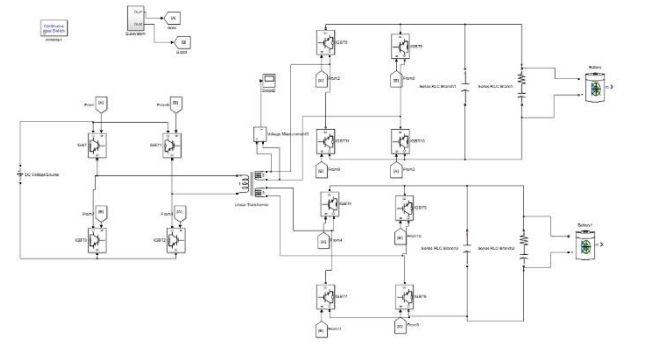

Figure 11: Simulink diagram of TAB converter

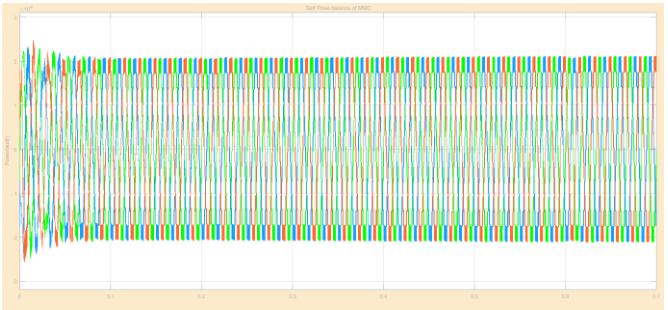

Figure 12:Self Power balance of TAB converter

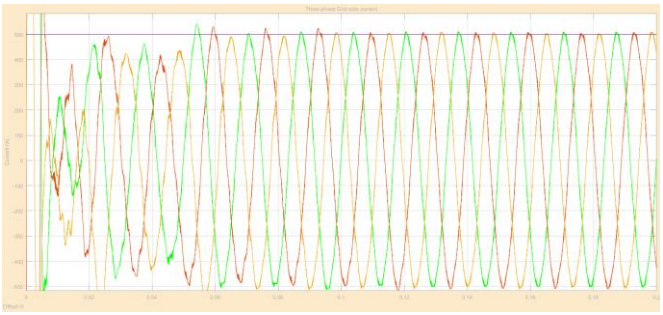

Figure 13: Three phase current

IV. DISCUSSION

The peoposed topology of TAB converter uses same method for DAB i.e.single phase shift (SPS) for the control. The simulation results demonstrate the viability of our suggested structure. In anticipation of future developments, the Multiport Triple Active Bridge (TAB) Converter exhibits favourable potential for Electric Vehicle (EV) charging stations. The multiport design of the system suggests a sophisticated approach to energy management, wherein power distribution is optimised across electric vehicles (EVs), batteries, and grids.

The introduction of bidirectional electricity flow inside the grid system facilitates enhanced stability. The adaptability of the TAB makes it well-suited for next-generation fast-charging solutions, allowing it to meet the diverse requirements of electric vehicles. The integration potential of Vehicle-to-Grid (V2G) technology has the capability to transform electric vehicles (EVs) into valuable resources for the electrical grid. It is anticipated that as technology advances, there will be improvements in efficiency and savings in costs. The implementation of standardisation initiatives contributes to the promotion of compatibility, while the integration of safety procedures enhances the resilience of systems. In summary, the trajectory of the TAB converter holds the potential to establish efficient, integrated, and sustainable electric vehicle charging ecosystems.

V. CONCLUSION

In conclusion, the incorporation of the Multiport Triple Active Bridge (TAB) Converter signifies a crucial development that has the capacity to greatly enhance the dependability of Electric Vehicle (EV) charging systems. The TAB converter addresses important issues by using its revolutionary multiport architecture. These challenges include the need to minimise the number of conversion stages, optimise energy distribution, decrease losses, and enable smooth integration of battery energy storage systems (BESS). The unique characteristics of the TAB converter promote a balanced and effective transfer of energy between electric vehicles (EVs), the grid, and the battery energy storage system (BESS), resulting in faster, more efficient, and reliable charging procedures.

In addition, the removal of superfluous conversion stages not only simplifies the system's structure but also enhances operational effectiveness and reduces expenses. The TAB converter is a crucial technology for enhancing the dependability of electric vehicle (EV) charging stations. It achieves this through its capacity to control power flow in both directions, incorporate fault tolerance mechanisms, and stabilise the grid.

In the current era characterised by the rapid growth of electric mobility, the significance of reliability becomes of utmost importance. The ability of the TAB converter to streamline complex system operations, enhance energy management, and enhance overall robustness is in perfect harmony with the changing requirements of this dynamic industry. The findings derived from this investigation emphasise the significance of integrating the TAB converter into electric vehicle (EV) charging systems, as it initiates a paradigm shift in the industry, leading to a future marked by resilient, effective, and environmentally-friendly charging infrastructure.

REFERENCES

[1] F. Hoffmann, J. Person, M. Andresen, M. Liserre, F. D. Freijedo and T. Wijekoon, "A Multiport Partial Power Processing Converter With Energy Storage Integration for EV Stationary Charging," in IEEE Journal of Emerging and Selected Topics in Power Electronics, vol. 10, no. 6, pp. 7950-7962, Dec. 2022, doi: 10.1109/JESTPE.2021.3102180.

[2] A. Hussain, V. Bui, and H. Kim, “Optimal sizing of battery energy storage system in a fast ev charging station considering power outages,” IEEE Transactions on Transportation Electrification, vol. 6, no. 2, pp. 453–463, 2020.

[3]] I. Lymperopoulos, F. A. Qureshi, A. Bitlislioglu, J. Poland, A. Zanarini, M. Mercangoez, and C. Jones, “Ancillary services provision utilizing a network of fast-charging stations for electrical buses,” IEEE

Transactions on Smart Grid, vol. 11, no. 1, pp. 665–672, Jan 2020

[4] T. S. Bryden, G. Hilton, B. Dimitrov, C. Ponce de Leon, and A. Cruden, “Rating a stationary energy storage system within a fast electric vehicle charging station considering user waiting times,” IEEE Transactions on Transportation Electrification, vol. 5, no. 4, pp. 879–889, 2019.

[5] E. Martinez-Laserna, E. Sarasketa-Zabala, I. Villarreal Sarria, D. Stroe, M. Swierczynski, A. Warnecke, J. Timmermans, S. Goutam, N. Omar, and P. Rodriguez, “Technical viability of battery second life: A study from the ageing perspective,” IEEE Transactions on Industry Applications, vol. 54, no. 3, pp. 2703–2713, May 2018.

[6] Y. Deng, Y. Zhang, and F. Luo, “Operational planning of centralized charging stations using second-life battery energy storage systems,” IEEE Transactions on Sustainable Energy, pp. 1–1, 2020.

[7] R. Chattopadhyay, G. Gohil, S. Acharya, V. Nair, and S. Bhattacharya, “Efficiency improvement of three port high frequency transformer isolated triple active bridge converter,” Conference Proceedings - IEEE Applied Power Electronics Conference and Exposition - APEC, vol. 2018-March, no. figure 1, pp. 1807–1814, 2018.

[8] Z. Wang and A. Castellazzi, “SiC-based Triple Active Bridge Converter for Shipboard Micro-grid Applications with Efficient Energy Storage,” 6th IEEE International Conference on Smart Grid, icSmartGrids 2018, pp. 39–45, 2019.

[9] Y. Tran, D. Dujic, and P. Barrade, “Multiport resonant dc-dc converter,” in IECON 2015 - 41st Annual Conference of the IEEE Industrial Electronics Society, 2015, pp. 003 839–003 844.

[10] K. Tomas-Manez, Z. Zhang, and Z. Ouyang, “Multi-port isolated llc resonant converter for distributed energy generation with energy storage,” in 2017 IEEE Energy Conversion Congress and Exposition (ECCE), 2017, pp. 2219–2226.

[11] F. Hoffmann, J. Lafrenz, M. Liserre, and N. Vazquez, “Isolated multiport converter as cost efficient solution for dc-fast charger of electric vehicle,” in IECON 2019 - 45th Annual Conference of the IEEE Industrial Electronics Society, vol. 1, 2019, pp. 4905–4910.

[12] F. Hoffmann, J. Lafrenz, M. Liserre, and N. Vazquez, “Multiwinding based semi-dual active bridge converter,” in 2020 IEEE Applied Power Electronics Conference and Exposition (APEC), 2020, pp. 2142–2149.

[13] C. Olalla, D. Clement, M. Rodriguez, and D. Maksimovic, “Architectures and control of submodule integrated dc–dc converters for photovoltaic applications,” IEEE Transactions on Power Electronics, vol. 28, no. 6, pp. 2980–2997, 2013.

[14] Karanayil B., Ciobotaru M., Agelidis V.G.: ‘Power flow management of isolated multiport converter for more electric aircraft’, *IEEE Trans. Power Electron.*, 2017, **32**, (7), pp. 5850 – 5861 (doi: https://doi.org/10.1109/TPEL.2016.2614019) .

[15] B. Zhao, Q. Song, W. Liu and Y. Sun, "A Synthetic Discrete Design Methodology of High-Frequency Isolated Bidirectional DC/DC Converter for Grid-Connected Battery Energy Storage System Using Advanced Components," in IEEE Transactions on Industrial Electronics, vol. 61, no. 10, pp. 5402-5410, Oct. 2014, doi: 10.1109/TIE.2014.2304915.

[16] J. R. R. Zientarski, M. L. da Silva Martins, J. R. Pinheiro, and H. L. Hey, “Evaluation of power processing in series-connected partial-power converters,” IEEE Journal of Emerging and Selected Topics in Power Electronics, vol. 7, no. 1, pp. 343–352, 2019.

[17] B. Zhao, Q. Song and W. Liu, "Efficiency characterization and optimization of isolated bidirectional dc–dc converter based on dual-phase-shift control for dc distribution application", *IEEE Trans. Power Electron.*, vol. 28, no. 4, pp. 1711-1727, Apr. 2013.

[18] C. Li, Y. E. Bouvier, A. Berrios, P. Alou, J. A. Oliver, and J. A. Cobos, “Revisiting ”partial power architectures” from the ”differential power” perspective,” in 2019 20th Workshop on Control and Modeling for Power Electronics (COMPEL), 2019, pp. 1–8.

[19] M. C. Mira, Z. Zhang, K. L. Jørgensen, and M. A. E. Andersen, “Fractional charging converter with high efficiency and low cost for electrochemical energy storage devices,” IEEE Transactions on Industry Applications, vol. 55, no. 6, pp. 7461–7470, 2019.

[20] K. Jørgensen, Z. Zhang, and M. Andersen, “Next generation of power electronic-converter application for energy-conversion and storage units and systems,” Clean Energy, vol. 3, no. 4, p. 307 315, 2019.